Available online at www.sciencedirect.com
SCIENCE DIRECT®
Microvascular Research xx (2004) xxx–xxx
MVR Microvascular Research
www.elsevier.com/locate/ymvre

Time response of interstitial fluid pressure measurements in cervix cancer

Houman Khosravani,[a] Brige Chugh,[b] Michael F. Milosevic,[c,d] and Kenneth H. Norwich[a,b,*]

[a] *Departments of Physiology and Physics, University of Toronto, Toronto, ON, Canada M5S 1A8*
[b] *Institute of Biomaterials and Biomedical Engineering, University of Toronto, Toronto, ON, Canada M5S 3G9*
[c] *Radiation Medicine Program, Princess Margaret Hospital, Toronto, ON, Canada M5G 2M9*
[d] *Department of Radiation Oncology, University of Toronto, Toronto, ON, Canada M5S 3E2*

Received 27 June 2003

Abstract

Increased interstitial fluid pressure (IFP) is a common finding in malignant tumors as a result of the abnormal tumor vasculature and a lack of functional lymphatics. A recent clinical study by Milosevic et al. [Cancer Res. 61 (2001) 6400] reported a link between elevated IFP and survival in patients with cancer of the cervix. Patients with high IFP were more likely to have recurrence of tumors even after radiotherapy and were also more likely to die of progressive disease, independent of other prognostic factors. In this complementary study, using human data, we analyze 152 cervical tumor pressure IFP measurements from 42 patients with clinically diagnosed cancer of the cervix, randomly selected from the sample of 102 patients involved in the original study. We propose a simple biophysical model, based on flow through porous media, to explain the time response of the measured pressure curves in human cervical tumors. The response of IFP was governed by a time-constant $\tau_{IFP} = 14 \pm 1$ s averaged over multiple tumor sites. Interstitial hydraulic conductivity was computed to be approximately equal to 4.3×10^{-6} cm^2/mm Hgs.

Keywords: Interstitial fluid pressure; Cervical cancer; Biophysics; Mathematical model

Introduction

Interstitial fluid pressure is elevated in most solid malignant tumors as a result of the abnormal tumor vasculature and a lack of functional tumor lymphatics (Baxter and Jain, 1989; Boucher and Jain, 1992; Leu et al., 2000). A clinical study by Milosevic et al. (2001) showed IFP to be an important prognostic factor in patients with cervix cancer who were treated with radiotherapy. IFP predicted local tumor control, the development of distant metastases, and overall patient survival independent of important clinical prognostic factors and tumor oxygenation. However, the biophysical mechanism underlying this important clinical observation is not understood. We develop a biophysical model with particular attention to the underlying tumor characteristics that influence interstitial fluid movement, and use this to describe the time-dependent changes in the IFP recordings that we observed in patients with cervix cancer. In addition, we analyze IFP pressure measurements from a representative subset of the cervical tumors that were included in the original study by Milosevic et al. (2001) with the aim to better understand the determinants governing elevated IFP in cervical tumor and their possible relation to patient outcome.

Clinical and experimental methods

The technique for measuring IFP in patients with cervix cancer has been described in detail previously (Milosevic et al., 1998, 2001). In brief, IFP was measured at examination under anesthesia with the patient in the lithotomy position. The cervix and tumor were visualized vaginally, and IFP was measured at one to five locations around the circumference of the tumor. At each location, the needle was first held at the elevation of the site of insertion until the pressure reading stabilized. The needle was then advanced 2 cm into the tumor. Clinical examination and staging using MRI were used to assure that the measurements were made in the central tumor and not inadvertently at the periphery or in surrounding normal tissue. Upon insertion, the needle was held in a fixed position until the pressure recording again stabilized (usually

* Corresponding author. Institute of Biomaterials and Biomedical Engineering, University of Toronto, 4 Taddle Creek Road, Toronto, Ontario, Canada M5S 3G9. Fax: +1-416-978-4317.
E-mail address: k.norwich@utoronto.ca (K.H. Norwich).

0026-2862/$ - see front matter © 2004 Elsevier Inc. All rights reserved.
doi:10.1016/j.mvr.2004.01.003

less than 60 s). A typical pressure tracing is shown in Fig. 1. The steady state IFP (SS-IFP) is defined as the difference between final plateau pressure within tumor and the calibrated zero point at the level of point of insertion. The IFP study (Milosevic et al., 1998, 2001) was approved by the Clinical Trials Committee of the Princess Margaret Hospital and the Human Subject Review Committee of the Office of Research Services at the University of Toronto. Written informed consent was obtained from each patient before measurements were taken.

Measurements were made using a modified wick-in-needle apparatus (Fadnes et al., 1977), comprised of a 22-gauge spinal needle with a length of 6.5 cm and internal diameter of 0.02 cm. A side port 2–4-mm long was custom-ground near the tip. The needle apparatus was connected to a piezoelectric pressure transducer using a 1-m polyethylene tube, with an internal diameter of 0.16 cm. The distal 1–2 cm of the needle was filled with multifilamentous cotton thread (to avoid occlusion and facilitate fluid flow once in tumor). The entire system was flushed with a heparin–saline solution to prevent clotting.

The time constant of the measurement system alone (needle and wick, polyethylene tubing, pressure transducer, and fluid) was evaluated using the ''pop test'' technique described by Milnor (1989) to assess sampling of sudden change in pressure. The system was filled with fluid and calibrated as for pressure measurement in a tumor. A balloon was placed over the end of the measurement needle and one of the ports of a stopcock, and secured in an airtight fashion. The balloon was inflated through the stopcock until the pressure in the system exceeded 500 mm Hg. After stabilization of the pressure recording, the balloon was burst, and the pressure response recorded. The time constant for the system was recorded to be the time required for the pressure to decline in magnitude by a factor of e^{-1}.

Pressure (IFP) response curves, in tumor, were fitted using a monoexponential function as suggested by the

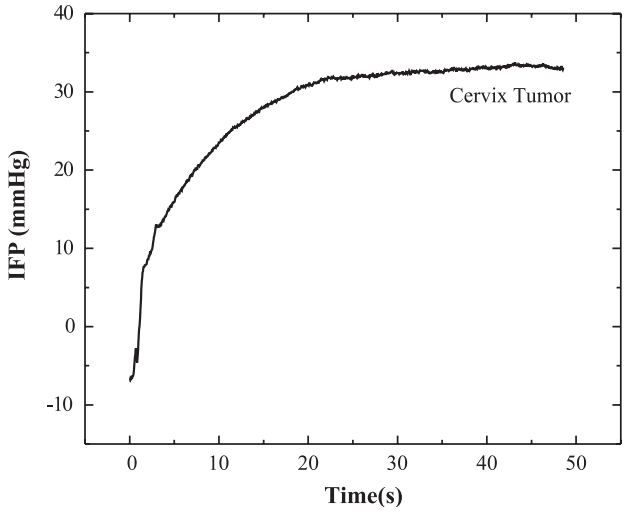

Fig. 1. Interstitial fluid pressure measurement in a cervix tumor.

mathematical model (see below). A standard least-squares routine, the Levenberg–Marquardt method (Press et al., 2002), was used. Specifically, the value of the merit function, χ^2, which represents the sum of the squares of the deviations of the theoretical curve from experimental data points, was minimized. Iterations were stopped when χ^2 reached a stable minimum value. For each IFP trace fitted, residual plots were constructed and inspected for lack of remaining trends; any tracings displaying a clear residual trend were excluded. These records were ones usually with significant movement artifact either upon insertion of the needle or due to the patient's breathing (oscillatory artifact). All recordings manifest a small degree of motion artifact upon needle insertion but not to a significant level (see Results).

Mathematical model

Fluid flow in the manometer

Interstitial fluid pressure recordings were obtained from multiple sites within the cervical tumors using a modified wick-in-needle technique (see Clinical and experimental methods). The pressure tracings represent the pressure that was recorded by the pressure transducer as a function of time after sudden insertion of the needle into the tumor. The shape and time response of the pressure tracing reflect the characteristics of both the measurement apparatus and the physical properties of the tissue near the needle. Insertion of the needle constitutes a sudden perturbation of the underlying steady state tumor environment, which may produce transient changes in the true IFP at the tip of the needle. Over time, IFP returns to its previous steady state value, which is determined mainly by the underlying capillary pressure (Baxter and Jain, 1989; Boucher and Jain, 1992). Our main interest was to obtain a physical description of the time-dependent change associated with fluid flow in the tumor and measurement apparatus from the moment of needle insertion into the tumor until a steady state IFP recording is established. Let us first consider the time constant associated with the needle apparatus.

The wick-in-needle is connected to the recording apparatus by a polyethylene tube that is noncompliant to the small amount of fluid being displaced as a result of the measurement (about 10 μl; Khosravani et al., 2003). The diameter of the tubing is four times that of the needle, and hence the needle is the primary site of any resistance to flow in the apparatus. Assuming laminar flow of fluid through the needle, we utilized Poiseuille's equation

$$Q = \frac{\Delta P \pi r^4}{8\eta L} \tag{1}$$

where Q is the flow rate, ΔP is the pressure gradient across the length of the needle, r is the radius of the needle, η is the kinematic viscosity, and L is the length of the needle. We

can also express this in terms of a generalized 'Ohm's law', $R = \Delta P / Q = 8\eta L / \pi r^4$. Assuming that effects such as resistances to flow and elastic compliance are negligible in other parts of the recording apparatus (e.g., tubing), we can consider the apparatus as a simple manometer (Fig. 2A). This is indeed a natural analogy since the needle and all its upstream connections are filled with saline. At the time of insertion of the needle into the tumor, the interstitial pressure, recorded by the manometer, is $\Delta P = p_1 - \rho g h$, where h is the height of the column of (passed) fluid (Fig. 2B, referring to the tubing structure on the left). Combining Ohm's expression for resistance with the difference in pressure as measured by the manometer, we obtain the following relation, which refers to the left-hand side of the apparatus in Fig 2B:

$$Q = \frac{1}{R}(p_1 - \rho g h) \tag{2}$$

Considering the flow, Q, through the needle to be a time-dependent function of the change of fluid height in the manometer, $Q = A\ \mathrm{d}h/\mathrm{d}t$, where A is the cross-sectional area of the needle. Hence, we obtain the following equation for the pressure, as measured by a change of height of the fluid in the manometer:

$$\frac{\mathrm{d}h}{\mathrm{d}t} + \frac{\rho g}{AR} h = \frac{p_1}{AR} \tag{3}$$

The above is a linear, first-order differential equation that is easily solved. The time constant governing the rise of fluid in the manometer is given by, $\tau_n = AR / \rho g$. This represents the product of the hydraulic resistance to fluid flow in the measurement needle (R), and the compliance of the measurement apparatus ($A / \rho g$) due to the column of water in the manometer. Using the dimensions of the needle ($r = 0.02$ cm, $L = 6.5$ cm), and assuming that the interstitial fluid as well as the fluid in the measurement system have characteristics of water ($\eta = 0.01$ poise and $\rho = 1.0$ g/cm^3), we find that, $\tau_n \sim 1.3$ s, $R = 776$ mm Hg s/cm^3 and $A / \rho g = 1.67 \times 10^{-3}$ cm^3/mm Hg.

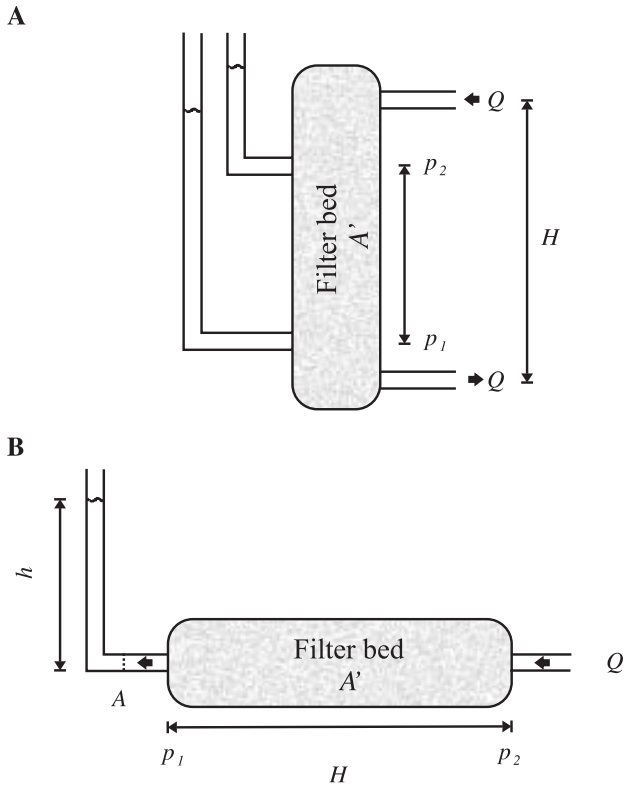

Fig. 2. Schematic representation of the model. (A) Classical paradigm for Darcy's law. Water enters at top right, percolates through the filter bed, and leaves at bottom right. The two tubes at the left are manometers. (B) Darcy paradigm rotated for application to fluid percolating through the interstitium of a tumor (filter bed). Fluid enters at right under pressure p_2, passes through tissue and emerges on the left at the needle under pressure, p_1. The horizontal segment of tubing at A represents the needle, attached to a vertical segment of tubing, representing the manometer. Fluid rises to height, h, in the manometer.

Fluid flow in the tumor interstitium

Let us now consider the behavior of the composite system comprised of the measurement apparatus and the tumor. The model of flow through tumor tissue is based on the following assumptions: (1) the trans-vascular resistance to fluid flow is much less than the interstitial resistance (Baxter and Jain, 1989), and (2) the tumor interstitium is relatively nonelastic, with the compliance of the needle tubing transducer being much more significant than that of the tumor, as elaborated on in the discussion below. Flow of fluid through the interstitium can be regarded as flow of fluid through a porous medium (Jain and Baxter, 1988), allowing for the use of Darcy's law (Scheidegger, 1974). In Darcy's original experiment (Fig. 2A) fluid passes through a filter bed, encapsulated in a vertical column, under the influence of gravity. The length of the porous filter bed is H and pressures p_1 and p_2 are measured at the top and bottom of the column, with Q the rate of flow and A', the cross-sectional area of the column. We utilize a modified version of Darcy's law, as stated by Scheidegger (1974):

$$Q = K' A' \frac{p_2 - p_1 + \rho |\vec{g}| H}{H} \tag{4}$$

where K' is a constant that incorporates the properties of the fluid and the porous medium, ρ is the density of the fluid and $\vec{g}$ is the acceleration due to gravity. K' is analogous to the interstitial conductivity coefficient, which is an important determinant of fluid dynamics in the interstitium of normal tissues and tumors (Baxter and Jain, 1989; Boucher et al., 1998). To apply Darcy's law to the percolation of interstitial fluid, we rotate Fig. 2A clockwise through 90° to obtain Fig. 2B. The filter bed now represents the tumor

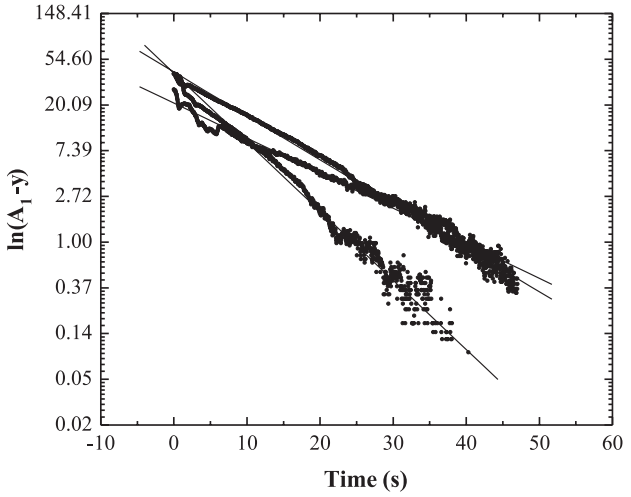

Fig. 3. Tumor interstitial pressure recordings, from three sites in the same patient, are fitted with a monoexponential function, $y = A_1 - A_2e^{-kt}$, here expressed as $\ln(A_{1\ -\ y}) = -kt + \ln(A_2)$. The slope of a linear fit ($r^2 > 0.97$ for all traces) to the pressure traces is a measure of the overall time constant (τ_{n+t}).

interstitium. That is, the cylinder of tissue that we model is taken to be in the horizontal plane, such that $|\vec{g}| \equiv |\vec{g}|\cos\theta$ with $\theta = \pi / 2$. Therefore, Darcy's law can be rewritten simply as

$$Q = \frac{K'A'}{H}(p_2 - p_1) \tag{5}$$

As expected, the above equation is similar to Pouseuille's law (Eq. (1)) since they describe similar processes (Scheidegger, 1974). The needle (manometer) measures the pressure at a depth of approximately 2 cm, and therefore, can be equated to p_1, as it appears in Eq. (3). By solving Eq. (5) for p_1, replacing Q by $A\ \mathrm{d}h / \mathrm{d}t$, and substituting into Eq. (3), we obtain

$$\frac{\mathrm{d}h}{\mathrm{d}t} = \frac{1}{AR}\left[p_2 - \frac{HQ}{K'A'} - \rho gh\right] \tag{6}$$

The above can then be rearranged into the standard form for a linear first-order differential equation

$$\frac{\mathrm{d}h}{\mathrm{d}t}\left[1 + \frac{R'}{R}\right] + \frac{\rho g}{AR}h = \frac{p_2}{AR} \tag{7}$$

where

$$R' = H/(K'A') \tag{8}$$

This differential equation is solved for $h(t)$ by standard methods to give

$$\rho gh(t) = p_2 + [\rho gh(0) - p_2]\exp\left[\frac{-\rho gt}{AR(1 + R'/R)}\right] \tag{9}$$

Replacing $\rho gh(t)$, the manometer pressure at time t, by $P_{\mathrm{IFP}}(t)$, and $\rho gh(0)$, the manometer pressure at zero time, by p_0, we can write

$$P_{\mathrm{IFP}}(t) = p_2 + [p_0 - p_2]\exp\left[\frac{-\rho gt}{AR[1 + R'/R]}\right] \tag{10}$$

$$\tau_{n\ +\ t} = \frac{A}{\rho g}[R + R'] \tag{11}$$

where the joint time constant for manometer plus tissue is represented by $\tau_{n\ +\ t}$. When time, t, becomes large, we see that P_{IFP} approaches a steady state value p_2, the pressure of interstitial fluid at the entrance to the tissue bed. This corresponds to the tumor microvascular pressure.

Results

The derived analytical expression for the time-dependent change in IFP toward steady state (Eq. 10) is a monoexponential function of the form $y = A_1 - A_2e^{-kt}$, where A_1, A_2, and k are computed constants used to fit the pressure traces. We define steady state IFP as the final steady state pressure minus the initially recorded pressure at the time of needle insertion into tissue, or in the nomenclature of Eq. (10)

$$\mathrm{IFP} = P_{\mathrm{IFP}} - p_0 \tag{12}$$

The curve in Fig. 3 can be interpreted in this manner.

The time-domain response of the measurement system alone to a sudden reduction of pressure (bursting the balloon) was characterized by a monoexponential decline in the recorded pressure with a time constant of 0.30 ± 0.05 s (mean ± standard deviation, $n = 6$). This is in good agreement with the model predictions, and provides further support indicating that the hydraulic resistance of the needle and tubing contributes only minimally to the overall time-response of the measurements in tumor.

Patients with cervix cancer were selected randomly from those who have undergone IFP recordings at Princess Margaret Hospital. Curve fitting of the patient data was performed using a least-squares algorithm (see Clinical and experimental methods) and final (steady state) IFP pressure and the time constant were computed for each pressure tracing. Multisite IFP pressure measurements from cervical tumors ($n = 152$, from 42 patients, average of three sites per

Table 1
Summary of observations from 42 patients with a total of 152 IFP pressure trace recordings selected randomly from the pool of patients involved in the study by Milosevic et al. (2001)

$N = 152$ sites, 42 patients (3 ± 1 sites/patient)	Mean of means ± SE	SD	Range
Steady state IFP (mm Hg)	22 ± 2	9	50
τ (s), IFP rise time	14 ± 1	9	44

Note that the two above variables, SS-IFP and τ, are not statistically correlated, $r = 0.09$, $P = 0.05$.

patient, minimum of 1), were fitted using a monoexponential function ($r^2 > 0.95$) for all curves analyzed (e.g., Fig. 3). Results are summarized in Table 1. Overall, the steady state IFP pressure was calculated to be 22 ± 2 mm Hg (mean of means:SE), ranging from IFP_{min} = 3 mm Hg to IFP_{max} = 80 mm Hg (Fig. 4A). This distribution of SS-IFPs is very similar to that presented in the original study (Milosevic et al., 1998), demonstrating that our random sample of patients is a valid representation of that population. The overall time constant 14 ± 1 s, ranging from $\tau_{(IFP)min}$ = 1 s to $\tau_{(IFP)max}$ = 78 s. We use the symbol τ_{IFP} to refer to the fitted value of the time constant, whereas τ_{n+t} refers to equivalent term as determined by the model. The large variability in τ_{IFP} is due to extensive heterogeneity in the composition and function of the interstitium, both within a tumor and between tumors in different patients (Fig. 4B). The mean of mean time constant, calculated by taking the mean of the means for each IFP tracing at multiple sites was 14 ± 1 s. No significant correlation was observed between the time constant and IFP at steady state, $r = 0.09$, $P = 0.05$ (Fig. 5). The patients randomly selected in this study were cross-checked with the list of patients in the survival study (Milosevic et

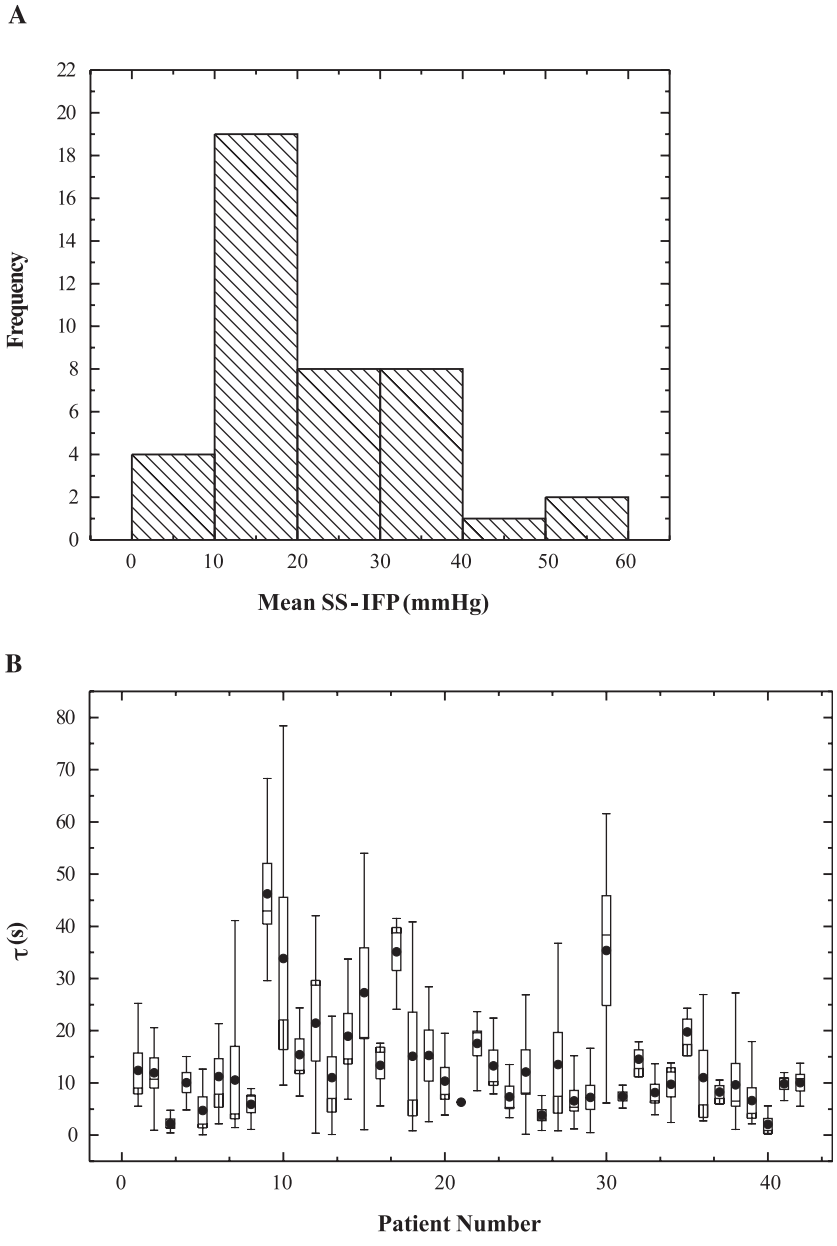

Fig. 4. Summary of steady state IFP (A) and time constants (B) as measured in 42 patients with cancer of the cervix. (A) Histogram of mean steady state IFP (SS-IFP) as calculated from multiple-site pressure recordings in tumor from each patient. Note that SS-IFPs are clearly elevated in this population of patients with cancer of the cervix. (B) Box plot of the calculated time constant (τ) values from multiple sites in each patients. The solid dot is the mean τ value over multiple sites, the surrounding vertical box spans the magnitude of the standard error, and the error bars the range of minimum and maximum values. Note the variation for each patient and across the series, with smaller time constants occurring more frequently.

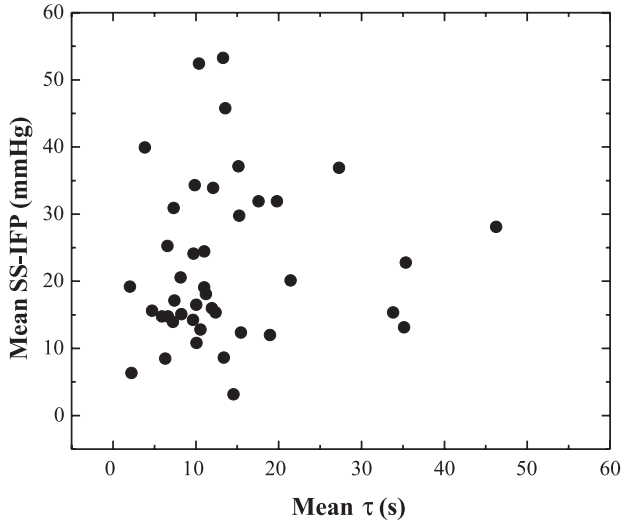

Fig. 5. Mean steady state IFP plotted vs. τ_{IFP} as computed for each patient across multiple sites of pressure recording. These observations do not display or suggest the existence of a linear relation (Pearson product moment, $r = 0.09$, $P > 0.05$). This lack of correlation persisted even if the data were plotted and analyzed without averaging for each patient.

al., 2001) and no association was found between computed values for the time constant, τ, and patient survival.

Using both our model and observations, we were able to estimate the order of magnitude of K', the hydraulic conductivity of the tumor interstitium, which directly influences the pressure measurement. Referring to Eq. (11), the time constant of the rise of interstitial pressure, τ_{n+t}, is given by the sum of two terms. However, we note that the magnitude of the first term, $AR / \rho g$, is about 1 s, so that the second term, $AR' / \rho g$, whose magnitude is about 10–20 s dominates. Using the explicit expression for R' (Eq. (8)), we can rewrite τ_{n+t} as

$$\tau_{n+t} \cong \frac{AR'}{\rho g} = \frac{A}{\rho g}\frac{H}{A'K'} \tag{13}$$

or

$$K' = \frac{A}{\rho g \tau_{n+t}}\frac{H}{A'} \tag{14}$$

The above equation can then be used to estimate the value of K' in tumor tissue. We represent the sampling volume of the needle, the region influencing the time-dependent measurement, as a cylinder of length H with sectional area A'. Bench-top experiments (Khosravani et al., 2003) in which colored ink was allowed to flow through the needle into a gel revealed that approximately 90% of the flow occurs through the side port of the needle.

We can now estimate the value of K' as follows. A = sectional area of needle bore = $\pi r^2 = 0.02^2\pi$ cm^2, $\rho = 1.0$ g/cm^3, $g = 980$ cm/s^2, and H, which is determined by the distance from the needle side port to the nearest capillaries, and is assumed to be 1/2 the average intercapillary distance, estimated as approximately 0.0025 cm (Netti et al., 1995). A' is determined by a circle with diameter equal the length of the needle side port (0.3 cm). $A' = 0.15^2\pi$; therefore,

$$K' = \frac{0.02^2\pi}{(1.0)(980)(14)}\frac{0.0025}{0.15^2\pi} = 3.24 \times 10^{-9}\text{cm}^4/(\text{dyn s}).$$

Since pressure of 1 mm of mercury is equal to $\rho_{merc}g(0.1) = 1323$ dyn/cm^2, $K' = 3.22 \times 10^{-9} \times 1323 = 4.286 \times 10^{-6}$ cm^2/mm Hg or about 4.3×10^{-6} cm^2/mm Hgs. Our estimation of K is similar to previously reported values (Boucher et al., 1998; DiResta et al., 1993; Guyton et al., 1966; Swabb et al., 1974).

Discussion

We used a randomly selected subset of interstitial fluid pressure (IFP) data, recorded from tumor in patients with diagnosed cancer of the cervix, to construct a simple biophysical model of fluid flow that underlies the time-dependent change observed during pressure recordings. The data were obtained from a prospective clinical study (Milosevic et al., 2001), which established a link between elevated tumor IFP and patient mortality. Elevated tumor IFP, independent of other clinical prognostic factors, determined patient survival. Clinically, the elevated steady state IFP is the prognostic factor; however, understanding underlying tissue properties governing the time-dependent IFP measurement may shed further light on causes of interstitial hypertension in cervical tumors. Our simple model, which takes into account the porous nature of the interstitium in a local region of tumor, resulted in a monoexponential function that was sufficient to describe the quantitative change in pressure, from the time of needle insertion into the tumor, to steady state IFP. We were also able to estimate the value of the interstitial hydraulic conductivity, $K' \sim 4.3 \times 10^{-6}$ cm^2/mm Hg·s.

The time-dependent behavior of IFP was recently investigated by Netti et al. (1995) in an ex vivo preparation. Their study examined the effects of microvascular pressure (MVP) and tumor blood flow (TBF) on IFP. They used a tissue-isolated tumor with a single artery and vein and altered flow conditions while monitoring IFP. In their comprehensive mathematical model, they demonstrated that fluid dynamics in the interstitium responded exponentially with two distinct time scales. The first response was found to be characteristic of the trans-capillary fluid exchange with a time constant of about 10 s. The second response was about 1000 s and resulted from percolation of fluid through the interstitial matrix after abrupt cessation of TBF. In this complementary study, we analyzed pressure tracings, recorded from patients with cancer of the cervix, obtained by sudden needle insertion into tumors. We

observed a mean time constant $\tau_{IFP} = 14 \pm 1$ s. For experimental determination of time constants, a function in the form of ($y = A_1 - A_2e^{-kt}$) was used, derived from basic principles of flow. Our model, deduced by simple considerations of the medium's macroscopic properties (see Eq. (10)) results in a function with the same experimentally validated shape (Netti et al., 1995).

In this model, we have ignored the compliance of the tumor interstitium, or its volume change per unit change in pressure, which is determined by the elasticity of the tissue. Although the tumor interstitium displays elastic properties, the compliance of the tissue volume sampled by the IFP measurement is probably small in comparison to the compliance of the manometer. There have been very few measurements of interstitial compliance in either tumor or normal tissue. Boucher et al. (1998) estimated tumor compliance to be about 50 μl/mm Hg for human tumor xenografts grown to volumes of between 0.2 and 0.5 cm^3. This translates to 0.1–0.25 cm^3/(mm Hg g) of tissue. Compliance values an order of magnitude smaller in the range of 0.01–0.05 cm^3/(mm Hg g) have been described for the skin and skeletal muscle of small mammals and rodents (Aukland and Reed, 1993). As previously discussed, the IFP sampling volume is small and confined to the tissue in the region of the needle side port. We estimate this to be 1.8×10^{-4} cm^3 for a needle port length of 0.3 cm and intercapillary distance of 0.0025 cm. Scaling the tumor and normal tissue compliance values above to correspond to the IFP sampling volume (assuming tissue density of 1 g/cm^3) yields values in the range of 1.8×10^{-6} to 4.5×10^{-5} cm^3/mm Hg, which are much smaller than the estimated manometer compliance of 1.67×10^{-3} cm^3/mm Hg.

We were able to estimate the value of K for cervix cancer using the time constant of the pressure recordings, τ_{IFP}, and assumptions about the sampling volume of the needle and the distribution of functional capillaries within this volume. We have no information about the characteristics of the vasculature in the region of the IFP measurements in individual tumors, so it was only possible to estimate K globally for the entire group of tumors using average values from the literature. A recent study by Boucher et al. (1998) offers an experimental avenue for directly measuring K. They recorded IFP in transplanted human adenocarcinoma in mice, using a two-needle approach: one needle infused fluid (radially) into the tumor, while another needle made a pressure measurement that was used to compute K (via Darcy's law). While experiments of this sort are feasible in the laboratory and provide valuable information about important tumor characteristics, they are much more difficult to implement clinically in a manner that yields reliable results.

The steady state IFP in tumors is determined by many factors, including the microvascular pressure, capillary hydraulic resistance, and interstitial resistance (Baxter and Jain, 1989). The latter is strongly influenced by the interstitial conductivity coefficient K. We note, from Eq. (14), that K is inversely proportional to the overall time constant, τ_{n+t}. Notwithstanding the fact that K in Eq. (14) also depends on the distribution of the vasculature in the region of the needle about which we had little information, our results suggest that variations in K from tumor to tumor exert a relatively small influence on the steady state IFP. This finding supports the idea that microvascular pressure and trans-capillary flow dominate the time-dependent behavior of IFP (Netti et al., 1995), rather than interstitial flow parameters within the tumor.

We regard our IFP recording as reflecting a local (regional) pressure measurement in heterogeneous tumor tissue characterized by physiological parameters that have both spatial and temporal components (Boucher et al., 1990; Eskey et al., 1992; Jain and Baxter, 1988; Mollica et al., 2003). Our study of human cervical tumors in vivo offers the advantage of direct evaluation of the pathophysiology. However, it limits our ability to access the entire spatial extent of the tumor, or to manipulate the tumor and its environment. Our simple model describes the overall shape of the pressure curve, in close agreement with experimental results and possibly further implicates the capillary pressure in driving the time response. Increased IFP in tumors is a common phenomenon in human and animal tumors (Guyton and Hall, 2000; Jain, 1988, 1987, 1990; Jain and Baxter, 1988; Stohrer et al., 2000). Increased IFP hinders drug delivery to tumors (Baxter and Jain, 1989; Boucher et al., 1998, 1990; Jain and Baxter, 1988); therefore, greater understanding of tissue properties and conditions leading to this condition are required to improve therapeutic modalities. In the case of cervical tumors, interstitial hypertension has been implicated as a significant predictor of patient mortality. A more detailed understanding of the biological mechanism underlying this association is essential if IFP is to be used as a guide to targeted cancer treatment in combination with radiation or chemotherapy. Knowledge of the complex tumor vascular structure, composition of the interstitium, and response of tumor cells to pressure changes will be important to furthering this goal.

Acknowledgments

This research has been supported by the National Cancer Institute of Canada, and by the Natural Sciences and Engineering Research Council of Canada.

References

Aukland, K., Reed, R.K., 1993. Interstitial–lymphatic mechanisms in the control of extracellular fluid volume. Physiol. Rev. 73, 1–78.

Baxter, L.T., Jain, R.K., 1989. Transport of fluid and macromolecules in tumors I: role of interstitial pressure and convection. Microvasc. Res. 37, 77–104.

Boucher, Y., Baxter, L.T., Jain, R.K., 1990. Interstitial pressure gradients in isolated tissue and subcutaneous tumors: implications for therapy. Cancer Res. 50, 4478–4484.

Boucher, Y., Jain, R.K., 1992. Microvascular pressure is the principal driving force for interstitial hypertension in solid tumors: implications for vascular collapse. Cancer Res. 52 (18), 5110–5114.

Boucher, Y., Brekken, C., Netti, P.A., Baxter, L.T., Jain, R.K., 1998. Intratumoral infusion of fluid: estimation of hydraulic conductivity and implications for the delivery of therapeutic agents. Br. J. Cancer 78 (11), 1442–1448.

DiResta, G.R., Lee, J., Larson, S.M., Arbit, E., 1993. Characterization of neuroblastoma xenograft in rat flank: I. Growth, interstitial fluid pressure, and interstitial fluid velocity distribution profiles. Microvasc. Res. 46 (2), 158–177.

Eskey, C.J., Koretsky, A.P., Domach, M.M., Jain, R.K., 1992. H-Nuclear magnetic resonance imaging of tumor blood flow: spatial and temporal heterogeneity in tissue-isolated mammary adenocarcinoma. Cancer Res. 52, 6010–6019.

Fadnes, H.O., Reed, R.K., Aukland, K., 1977. Interstitial fluid pressure in rats measured with a modified wick technique. Microvasc. Res. 14, 27–36.

Guyton, A.C., Hall, J.E., 2000. Textbook of Medical Physiology, tenth ed. W.B. Saunders, London.

Guyton, A.C., Scheel, K., Murphree, D., 1966. Interstitial fluid pressure III. Its effect on resistance to tissue fluid mobility. Circ. Res. 19, 412–419.

Jain, R.K., 1987. Transport of molecules in the tumor interstitium: a review. Cancer Res. 47 (12), 3039–3051.

Jain, R.K., 1988. Determinants of tumor blood flow: a review. Cancer Res. 48 (10), 2641–2658.

Jain, R.K., 1990. Physiological barriers to delivery of monoclonal antibodies and other macromolecules in tumors. Cancer Res. 50, 814–819.

Jain, R.K., Baxter, L.T., 1988. Mechanisms of heterogeneous distribution of monoclonal antibodies and other macromolecules in tumors: significance of elevated interstitial pressure. Cancer Res. 48 (24 Pt 1), 7022–7032.

Khosravani, H., Milosevic, M.F., Norwich, K.H., 2003. Bench-top experiments using a water column as a steady pressure source, an albumin laden SDS-PAGE gel as a model of a tissue-like porous medium, and identical IFP measurement needle were used to approximate the amount of fluid flow over 15 s interval for a pressure source of 30 mm Hg. To the water ink was added to allow for visualization of fluid distribution entering the gel (unpublished observations).

Leu, A.J., Berk, D.A., Lymboussaki, A., Alitalo, K., Jain, R.K., 2000. Absence of functional lymphatics within a murine sarcoma: a molecular and functional evaluation. Cancer Res. 60 (16), 4324–4327.

Milnor, W.R., 1989. Hemodynamics, second ed. Williams & Wilkins, Baltimore, p. 312.

Milosevic, M.F., Fyles, A.W., Wong, R., Pintilie, M., Kavanagh, M.C., Levin, W., Manchul, L.A., Keane, T.J., Hill, R.P., 1998. Interstitial fluid pressure in cervical carcinoma: within tumor heterogeneity, and relation to oxygen tension. Cancer 82 (12), 2418–2426.

Milosevic, M., Fyles, A., Hedley, D., Pintilie, M., Levin, W., Manchul, L., Hill, R., 2001. Interstitial fluid pressure predicts survival in patients with cervix cancer independent of clinical prognostic factors and tumor oxygen measurements. Cancer Res. 61 (17), 6400–6405.

Mollica, F., Netti, P.A., Jain, R.K., 2003. A model for temporal heterogeneities of tumor blood flow. Microvasc. Res. 65, 56–60.

Netti, P.A., Baxter, L.T., Boucher, Y., Skalak, R., Jain, R.K., 1995. Time dependent behavior of interstitial fluid pressure in solid tumors: implications for drug delivery. Cancer Res. 55 (22), 5451–5458.

Press, W.H., Teukolsky, S.A., Vetterling, W.T., Flannery, B.P., 2002. Numerical Recipes in C++: The Art of Scientific Computing. Cambridge Univ. Press, New York.

Scheidegger, A.E., 1974. The Physics of Flow Through Porous Media. University of Toronto Press, Toronto.

Stohrer, M., Boucher, Y., Stangassinger, M., Jain, R.K., 2000. Oncotic pressure in solid tumors is elevated. Cancer Res. 60 (15), 4251–4255.

Swabb, E.A., Wei, J., Gullino, P.M., 1974. Diffusion and convection in normal and neoplastic tissues. Cancer Res. 34, 2814–2822.